Available online at www.sciencedirect.com
ScienceDirect
Catalysis Today 127 (2007) 304–318
CATALYSIS TODAY
www.elsevier.com/locate/cattod

Mechanistic aspects of the water–gas shift reaction on alumina-supported noble metal catalysts: *In situ* DRIFTS and SSITKA-mass spectrometry studies

George G. Olympiou, Christos M. Kalamaras, Constantinos D. Zeinalipour-Yazdi, Angelos M. Efstathiou *

Department of Chemistry, Heterogeneous Catalysis Laboratory, University of Cyprus, P.O. Box 20537, CY 1678 Nicosia, Cyprus

Available online 15 June 2007

Abstract

Steady-state isotopic transient kinetic analysis (SSITKA) experiments coupled with mass spectrometry were performed *for the first time* to study essential mechanistic aspects of the water–gas shift (WGS) reaction over alumina-supported Pt, Pd, and Rh catalysts. In particular, the concentrations (μmol g^{-1}) of *active intermediate species* found in the carbon-path from CO to the CO_2 product gas (use of ^{13}CO), and in the hydrogen-path from H_2O to the H_2 product gas (use of D_2O) of the reaction mechanism were determined. It was found that by increasing the reaction temperature from 350 to 500 °C the concentration of active species in both the carbon-path and hydrogen-path increased significantly. Based on the large concentration of active species present in the hydrogen-path (OH/H located on the alumina support), the latter being larger than six equivalent monolayers based on the exposed noble metal surface area ($\theta > 6.0$), the small concentration of OH groups along the periphery of metal-support interface, and the significantly smaller concentration (μmol g^{-1}) of active species present in the carbon-path (adsorbed CO on the noble metal and COOH species on the alumina support and/or the metal-support interface), it might be suggested that diffusion of OH/H species on the alumina support towards catalytic sites present in the hydrogen-path of reaction mechanism might be considered as a slow reaction step. The formation of labile OH/H species is the result of dissociative chemisorption of water on the alumina support, where the role of noble metal is to activate the CO chemisorption and likely to promote formate decomposition into CO_2 and H_2 products. It was found that there is a good correlation between the surface concentration and binding energy of CO on the noble metal (Pt, Pd or Rh) with the activity of alumina-supported noble metal towards the WGS reaction.

Keywords: Water–gas shift reaction; Supported-noble metal catalysts; SSITKA; DRIFTS; TPD; Catalytic reaction mechanisms

1. Introduction

The heterogeneously catalyzed water–gas shift (WGS) reaction,

$$CO + H_2O \leftrightarrow CO_2 + H_2 \quad (\Delta H^{\circ}_{298\,K} = -41\,kJ/mol) \qquad (1)$$

has historically been an important industrial chemical process in the ammonia synthesis, the hydro-processing of petroleum, and the production of hydrogen via steam reforming of hydrocarbons [1]. In recent years, there has been a renewed interest in the WGS reaction due to the need for low-cost pure hydrogen production by further developments of hydrocarbon steam-reforming technologies in which natural gas and other biomass-derived liquid fuels, such as ethanol, sugars and bio-oil can efficiently be used to produce syngas and hydrogen [2–5]. In addition, WGS reaction is essential for hydrogen-operated fuel cell power generation systems for which the CO concentration in the fuel must be less than 10 ppm [6].

Nowadays, the WGS reaction is one of the primary industrial reactions that produce H_2 and some sources predict that until 2030, 10% of the yearly consumption of energy will originate from the WGS reaction [7]. Commercially, the reduction in the CO content of syngas is achieved in a two-step process that involves a high- and a low- temperature water–gas shift reaction, known as ''HTS'' and ''LTS'' processes, respectively. In the first step, carried out in the ~310–450 °C range with the

* Corresponding author. Tel.: +357 2 2892776; fax: +357 2 2892801.
E-mail address: efstath@ucy.ac.cy (A.M. Efstathiou).

0920-5861/$ – see front matter © 2007 Elsevier B.V. All rights reserved.
doi:10.1016/j.cattod.2007.05.002

use of Fe_3O_4/Cr_2O_3 catalysts, the CO concentration is reduced from 10 to 3 vol%. In the second step carried out in the ~180–250 °C range, the CO content is further reduced to 500 ppm with the use of $Cu/ZnO/Al_2O_3$ catalysts [8–10]. These catalysts are pyrophoric and deactivate if exposed to air and condensed water [10]. Attempts now are focused in finding noble metals-, Au- and Cu-based catalysts of low loading that are non-pyrophoric with high activity at low-temperatures and which will lower the CO content of hydrogen gas stream produced in steam reforming of hydrocarbons technologies to concentrations less than 5 ppm [5,9].

A number of different mechanisms for the WGS reaction over metal oxides have been proposed and disagreements exist about the important active intermediate species involved and the rate-determining step [11,12]. Several mechanistic studies that examined the water–gas shift reaction on metal oxides and supported-metal catalysts made use of the *in situ* DRIFTS technique. Shido et al. examined MgO [13], ZnO [14], CeO_2 [15], and Rh supported on doped-CeO_2 [16] catalysts. They found that the WGS reaction proceeds through a surface *formate* (–COOH) species being an important active reaction intermediate. Similar conclusions were drawn by Chenu et al. [17] over Pt/MgO and Pt/ZrO_2 catalysts, Jacobs et al. [18] over Pt/CeO_2 at high H_2O/CO ratios, and by Grenoble et al. [19] over alumina-supported Pt, Pd, Rh, and other group VIIB, VIII, and IB metals.

Steady-state isotopic transient kinetic analysis (SSITKA) has long been documented and widely accepted as one of the most powerful techniques to elucidate in a rigorous manner mechanisms of heterogeneous catalytic reactions [20]. For the present catalytic system, only few studies were reported dealing with the application of SSITKA technique. The *reverse WGS* reaction in the absence of water over a Pt/CeO_2 catalyst was studied by Tibiletti et al. [21] and Goguet et al. [22] by SSITKA-DRIFTS. It was found that the main active intermediate for the formation of CO was *carbonate*, and that surface *formate* (–COOH) would rather be considered as a spectator species. Jacobs et al. [11,23] investigated the low-temperature (225 °C) *forward WGS* reaction over the same catalyst by SSITKA-DRIFTS. It was confirmed that the exchange rate of formate and carbonates was the same, and, therefore, formate was considered as an active intermediate of the WGS reaction as opposed to the case of reverse WGS reaction [21,22].

In the present work, for *the first time* the SSITKA-mass Spectrometry technique was applied *to quantify* the active ''carbon-containing'' (use of ^{13}CO) and ''H-containing'' (use of D_2O) intermediate species formed during the WGS reaction at 350 and 500 °C over Pt, Pd, and Rh supported on γ-Al_2O_3 of similar noble metal dispersion. Thus, the effect of the chemical nature of the noble metal used on the important kinetic parameter of surface concentration of active intermediate species was studied. The measurement of a large concentration ($\mu mol\ g^{-1}$) of active ''H-containing'' (e.g., OH, H) species and a significantly smaller concentration of active ''C-containing'' (e.g., HCOO, CO) species established under steady state reaction conditions, and the estimation also of a small concentration of OH groups along the periphery of metal-support interface, allows to suggest that surface diffusion of H/OH species present on the alumina support towards catalytic sites to form active adsorbed formate (HCOO) species residing on the alumina support and/or the metal-support interface might be considered as an important slow step of the WGS reaction. It is suggested that noble metal is necessary to activate CO chemisorption, and likely to promote formate decomposition into H_2 and CO_2 products. It was found that the active ''carbon-containing'' intermediate species at 350 °C is less than 0.1 of an equivalent monolayer based on the noble metal surface area, and larger than one monolayer at 500 °C. The latter result provides evidence for the presence of an active ''carbon-containing'' intermediate species (e.g., formate) on the alumina surface and/or along the periphery of metal-support interface.

2. Experimental

2.1. Catalyst preparation

The three noble metal (Pt, Pd, Rh) alumina-supported catalysts (0.5 wt%) were prepared by impregnating γ-alumina (5.8 nm mean pore diameter, 148 $m^2\ g^{-1}$, 150 mesh particle size) with an aqueous solution of $Pt(NH_3)_2(NO_2)_2$, $Rh(NO_3)_3$ and $Pd(NO_3)_2 \times H_2O$ (Aldrich) for Pt, Rh and Pd metals, respectively. A given amount of precursor solution corresponding to the desired 0.5 wt% metal loading was used to impregnate the alumina support at 50 °C for 6 h. The resulting slurry was dried at 120 °C overnight. Prior to any catalytic measurements the fresh catalyst sample was calcined in a 20% O_2/He (50 NmL min^{-1}) gas mixture at 500 °C for 2 h and then reduced in pure H_2 at 300 °C for 2 h.

2.2. Catalyst characterization

2.2.1. H_2 and CO temperature-programmed desorption (TPD) experiments

The dispersion of noble metals in the catalysts was determined by selective H_2 chemisorption at 25 °C followed by TPD according to the procedures described elsewhere [24]. Activated hydrogen chemisorption [25] was noticed in the case of Pt/γ-Al_2O_3 and Rh/γ-Al_2O_3 catalysts, and this was taken into account for estimating metal dispersion. More precisely, following H_2 adsorption at 200 °C, the catalyst was cooled to 25 °C in H_2/He flow and then purged in He flow for 5 min before TPD. In the case of Pd/γ-Al_2O_3 catalyst, metal dispersion was estimated after following the experimental procedure suggested by Aben [26] to avoid formation of PdH_x. More precisely, hydrogen chemisorption was conducted at 70 °C using a 1300 ppm H_2/He gas mixture before TPD.

CO TPD experiments were performed following chemisorption of CO at 25 °C. All TPDs were performed in a specially designed gas flow system previously described [27] using 0.3 g of catalyst sample, 30 NmL min^{-1} of He flow rate, and 30 °C min^{-1} of heating rate. Quantitative analysis of the effluent gas stream of micro-reactor was done with an *on line*

quadrupole mass spectrometer (Omnistar, Balzers) equipped with a fast response inlet capillary/leak valve (SVI050, Balzers) and data acquisition systems. The mass numbers (m/z) 2, 18, 28, 32, 44 used for H_2, H_2O, CO, O_2 and CO_2, respectively, were continuously monitored. The gaseous responses obtained by mass spectrometry were calibrated against standard mixtures. The accuracy of quantitative analysis of TPD response curves was within 3% for H_2, CO, CO_2 and O_2. No attempts were made to quantify the water signal. For the TPD runs, the fresh catalyst sample was first oxidized in 20% O_2/He at 600 °C for 2 h, and then reduced in 10% H_2/He at 300 °C for 2 h. The catalyst was then purged in He flow at 500 °C until no H_2 evolution was observed. It was then quickly cooled to room temperature.

2.3. In situ DRIFTS studies

2.3.1. CO chemisorption

A Perkin-Elmer Spectrum GX II FTIR spectrometer equipped with a high-temperature/high-pressure temperature controllable DRIFTS cell (Harrick, Praying Mantis) were used to *in situ* record spectra obtained under different reaction conditions. The spectrum of the solid catalyst taken in Ar flow at the desired reaction temperature, following catalyst pretreatment (20% O_2/Ar at 500 °C for 2 h followed by pure H_2 at 300 °C for 2 h) was subtracted from the spectrum of the catalyst exposed to the reaction mixture. In the case of CO chemisorption, the catalyst sample in a very fine powder form was diluted with dry KBr (1:5 w/w) for improved signal-to-noise ratio. Signal averaging was set to 40 scans per spectrum and the spectra were collected at the rate of 1 scan/s at a 2 cm^{-1} resolution in the 4000–800 cm^{-1} range. DRIFTS spectra when necessary were smoothed to remove high frequency noise and further analyzed using the software Spectrum® for Windows. Deconvolution of the thus derived DRIFTS spectra was performed according to reported guidelines [28]. CO chemisorption (0.5 vol% CO/He) was performed at 25 °C.

2.3.2. Water–gas shift reaction

The apparatus used to perform the WGS reaction in the DRIFTS cell consisted of an HPLC pump (GILSON 307) used for the supply of liquid water. The latter was first passed through a coil evaporator and then mixed with CO and Ar gases in a mixing chamber. The flow rate of a given feed gas was controlled via thermal mass flow control (MFC) valves (MKS Instruments, model 247C). The gas lines leading to and from the DRIFTS cell were heat traced and insulated with general purpose insulating wrap. The temperature of the gas lines was kept at $T > 200$ °C. The effluent stream from the DRIFTS cell could also be directed to a mass spectrometer for *operando* spectroscopic studies. Further details are provided elsewhere [29]. The reaction feed composition used was 3 vol% CO/12.5 vol% H_2O/84.5 vol% Ar at a total flow rate of 100 NmL/min.

2.4. Steady state catalytic measurements

Steady-state catalytic measurements were carried out on a Micro-reactivity Pro apparatus (CSIC, Spain) and in the experimental set-up previously described in detail [30]. The reaction feed composition was 3 vol% CO/10 vol% H_2O/87 vol% He at a total flow rate of 200 NmL/min. The catalyst particle size was between 0.1 and 0.2 mm. The amount of catalyst sample used for each catalyst composition was 0.5 g and the GHSV was kept constant at 45,000 h^{-1} in all catalytic measurements. The effluent stream from the reactor was directed to a mass spectrometer (Omnistar, Balzer) for *on line* measurements of H_2, CO and CO_2. The purity of the gases used in the catalytic experiments (e.g., H_2, He, CO, Ar) all provided by Linde was higher than 99.95%.

2.5. SSITKA-mass spectrometry studies

The isotopes used in the SSITKA experiments were ^{13}CO (99.5 atom% ^{13}C, Spectra Gases) and deuterium oxide (D_2O) (99.96 atom% D, Aldrich). SSITKA experiments were performed using two HPLC pumps (GILSON 307) for the addition of H_2O and D_2O to the reactor feed stream in the apparatus described in Section 2.4. SSITKA experiments performed in order to follow the ''hydrogen-path'' of reaction involved the switch 3% CO/10% H_2O/Ar/Kr (30 min, T) → 3% CO/10% D_2O/Ar (T, t) at T = 350 and 500 °C, while those to follow the ''carbon-path'' of reaction involved the switch 3%^{12}CO/10% H_2O/Ar/He (30 min, T) → 3%^{13}CO/10% H_2O/Ar (T, t). The dry gas from the exit of a condenser placed downstream the reactor was directed to the mass spectrometer for *on line* recording of H_2, CO and CO_2 normal and isotope-containing (D, ^{13}C) species [30]. Calibration of D_2 response was made using a 5% D_2/Ar (Spectra Gases) calibration gas mixture. The mass of alumina-supported noble metal catalyst was adjusted so as to keep the CO conversion below 20%. The total mass of the catalytic bed material was kept to 0.5 g (catalyst diluted with silica). Data acquisition with mass spectrometer was performed at a scan rate of 50 ms per cycle (five pre-selected appropriate mass numbers were used).

3. Results and discussion

3.1. Catalytic activity studies

The effect of reaction temperature on the activity (CO conversion) of the three alumina-supported noble metal catalysts towards the WGS reaction is presented in Fig. 1. The catalytic behavior of γ-Al_2O_3 alone is also shown. The conversion of carbon monoxide due to the WGS reaction is given by:

$$X_{CO} = \frac{(F_{CO}^{in} - F_{CO}^{out})}{F_{CO}^{in}} \quad (2)$$

where F_{CO}^{in} and F_{CO}^{out} are the molar flow rates (mol min^{-1}) of CO at the reactor inlet and outlet, respectively. For comparison, the CO conversion at thermodynamic equilibrium (X_{eq}, Fig. 1) is also given. The thermodynamic equilibrium curve is described

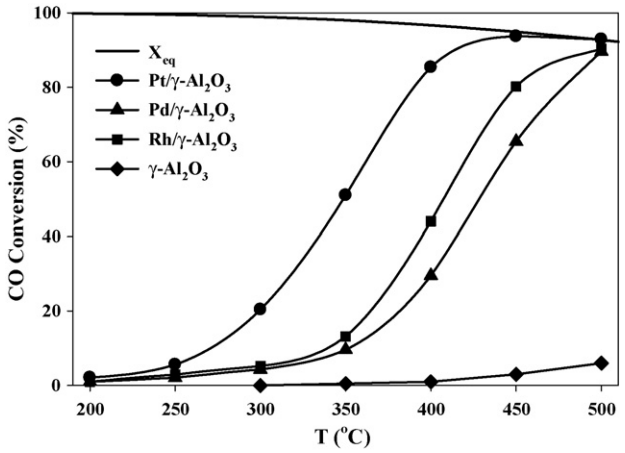

Fig. 1. Effect of WGS reaction temperature on the conversion of CO obtained over Pt, Pd and Rh (0.5 wt%) supported on γ-Al_2O_3. Also shown is the CO conversion (X_{eq}) vs. T curve for equilibrium conditions ($y^{in}_{CO} = 0.03$ and $y^{in}_{H_2O} = 0.1$). Experimental conditions: catalyst mass, $W = 0.5$ g; feed composition: 3% CO/10% H_2O/He; total flow rate, $Q = 200$ NmL min^{-1}.

by the following relationship:

$$\frac{(y^{in}_{CO}X_{eq})^2}{(y^{in}_{CO} - y^{in}_{CO}X_{eq})(y^{in}_{H_2O} - y^{in}_{CO}X_{eq})} = \exp\left(\frac{4577.8}{T} - 4.33\right) \quad (3)$$

where y^{in}_{CO} (0.03) and $y^{in}_{H_2O}$ (0.1) are the molar fractions of CO and H_2O in the feed stream, respectively. This curve was derived using the equilibrium constant (K_{eq}) values reported [31] and appropriate mass balances. The curve shows that below 260 °C full CO conversion is achieved. A decrease in the CO conversion by 7.3 percentage units is noticed at 500 °C.

The catalytic activity of the alumina-supported noble metals follows the order: Pt ≫ Rh > Pd in the 300–500 °C range investigated (Fig. 1), with Pt being significantly more active than the other two metals. These results are in excellent agreement with those reported by Panagiotopoulou and Kondarides [32,33] who examined the WGS reaction (same feed composition) over various noble metals supported on reducible (TiO_2, CeO_2, La_2O_3, YSZ) and irreducible (SiO_2, MgO, γ-Al_2O_3) metal oxides. It is noted at this point that the noble metal dispersion of the three catalysts was found to be 48, 47, and 52%, respectively, for the 0.5 wt% Pt/γ-Al_2O_3, 0.5 wt% Rh/γ-Al_2O_3, and 0.5 wt% Pd/γ-Al_2O_3 catalysts. Thus, metal particle size effects might be neglected in explaining the observed activity differences of the three supported-noble metal catalysts. In fact, Panagiotopoulou and Kondarides [33] reported that the WGS reaction investigated is *structure-insensitive* in the case of Pt/γ-Al_2O_3 catalyst ($1.0 < d_{Pt} < 7.1$ nm).

Panagiotopoulou and Kondarides [33] reported that the apparent activation energy of the WGS reaction depends significantly on the nature of noble metal. In particular, values of 24.9, 27.9, and 18.4 kcal mol^{-1}, respectively, were reported for Pt, Rh, and Pd alumina-supported catalysts. Taking into account the results of Fig. 1, it appears that the order of activity must strongly depend on other kinetic parameters, such as the concentration of active intermediate species that are found in the "carbon-path" and "hydrogen-path" of the reaction mechanism. This aspect is presented and discussed next and provides explanations for the activity order observed (Fig. 1).

The CO conversion over the γ-Al_2O_3 support alone is practically zero in the 200–400 °C range. At $T > 400$ °C, a measurable activity is observed. For example, at 500 °C a CO conversion of 6% was obtained (Fig. 1). This result agrees with the SSITKA results presented next, where at 500 °C the concentration of active carbon-containing intermediate species formed during reaction is larger than one equivalent monolayer, based on the noble metal surface area, suggesting that at least part of these active carbon-containing species must reside on the γ-alumina support. It will also be shown next that a large concentration of surface hydroxyl (–OH) groups and H species residing on the alumina support surface participate in the reaction path from H_2O to the formation of H_2(g) during the WGS reaction.

3.2. Mechanistic studies (SSITKA-mass spectrometry)

3.2.1. Determination of "H-pool"

The SSITKA technique [20] was used to follow the hydrogen-path, named "H-path" of the WGS reaction mechanism from H_2O to the H_2 product gas under kinetic regime conditions ($X_{CO} < 20\%$) following the switch 3% CO/10% H_2O/Ar/Kr (30 min, T) → 3% CO/10% D_2O/Ar (T, t) at $T = 350$ and 500 °C. Fig. 2 presents the transient concentration response curves of H_2, HD, D_2 and Kr obtained after the isotopic switch was made over the Pt/γ-Al_2O_3 catalyst at 350 (Fig. 2a) and 500 °C (Fig. 2b). The CO conversion was 20 and 11%, respectively at 350 and 500 °C. The Kr response curve describes the hydrodynamic behavior of the flow-system from the chromatographic switching valve to the mass spectrometer (through the reactor with the catalyst in place), and accounts for the gas hold-up in the gas lines and the reactor volume [20]. Details of the proper experimental precautions to be taken for accurate performance of the SSITKA technique and the recording of transient response curves was reported [20]. The transient response curves shown in Fig. 2 and the quantitative results obtained were reproducible with less than 5% error after performing consecutive switches between the CO/H_2O/Ar/Kr and CO/D_2O/Ar gas mixtures. The concentration of active "H-containing" intermediate species ("H-pool") that are found in the mechanistic "H-path" of the WGS reaction is estimated based on the transient response curves of H_2, HD and Kr via the following relationship:

$$N_H\,(\mu\text{mol H}/g_{cat}) = \left(\frac{F_T}{W}\right)\left[2\int_0^{t^f}(y_{H_2} - y_{Kr})\,dt + \int_0^{t^f} y_{HD}\,dt\right] \quad (4)$$

where, y_i is the molar fraction (ppm) of the gas phase species i, F_T is the total molar flow rate (mol min^{-1}) at the reactor outlet,

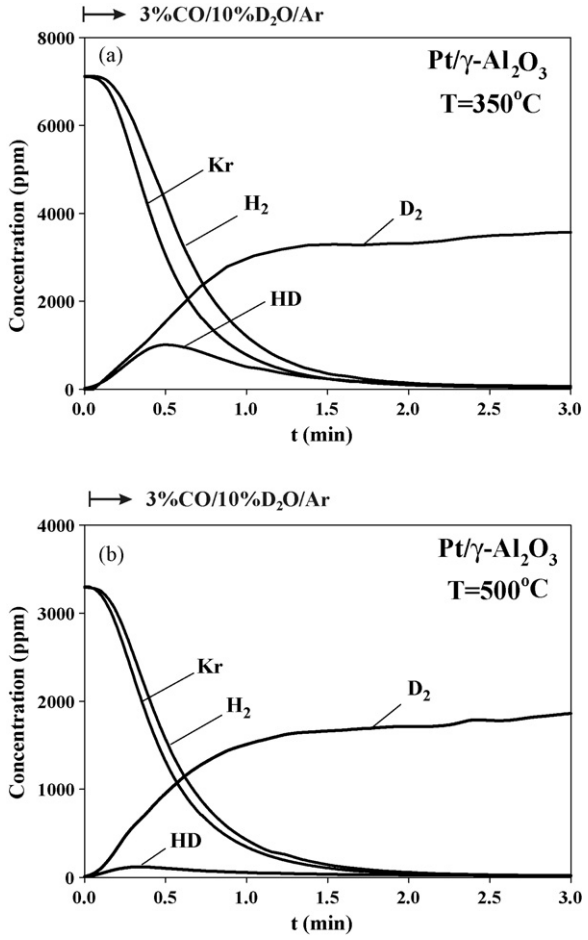

Fig. 2. SSITKA-mass spectrometry experiments performed to follow the ''H-path'' of WGS reaction over Pt/γ-Al_2O_3 at (a) 350 and (b) 500 °C, according to the gas delivery sequence: 3% CO/10% H_2O/Ar/Kr (30 min) → 3% CO/10% D_2O/Ar (t).

W is the mass of catalyst (g), and t^f is the time (min) required to obtain the new steady-state after the isotopic switch.

The size of the surface ''H-pool'' (μmol H g_{cat}^{-1}) estimated is reported in Table 1 within 5% of accuracy. In Table 1 a corresponding equivalent surface coverage of ''hydrogen-containing'' species (θ_H) is tabulated after using the noble metal dispersion (%D) of each catalyst. The accuracy of these values is considered to be within 5–10%. The surface coverage of ''hydrogen-containing'' species in all cases was found to be significantly larger than one ($\theta_H \gg 1$), which implies that most of the concentration of these species is present on the surface of γ-alumina. The nature of these species is labile hydroxyl groups (–OH) and H species. The latter are formed after water dissociation on the surface of γ-alumina (see details in Section 3.4). Since γ-Al_2O_3 is a non-reducible metal oxide, in order that both water dissociation on alumina and a complete catalytic cycle can take place, both H and OH species must participate in the reaction mechanism to form CO_2 and H_2 [34].

Table 1
Concentration (μmol g_{cat}^{-1}) of active ''H-containing'' (H-pool) and ''C-containing'' (C-pool) adsorbed surface reaction intermediates accumulated under steady-state WGS reaction conditions over Pt, Rh and Pd (0.5 wt%) supported on γ-Al_2O_3 measured by SSITKA-mass spectrometry

Catalyst	T (°C)	H-pool (μmol g_{cat}^{-1}) or (θ)[a]	C-pool (μmol g_{cat}^{-1}) or (θ)[a]
0.5 wt% Pt/γ-Al_2O_3	350	350 (28.5)	1.3 (0.1)
	500	1664 (135.6)	31.7 (2.6)
0.5 wt% Pd/γ-Al_2O_3	350	235 (9.8)	0.5 (0.02)
	500	3194 (132.7)	28.6 (1.2)
0.5 wt% Rh/γ-Al_2O_3	350	138 (6.2)	2.4 (0.1)
	500	1093 (49.0)	27.3 (1.2)

[a] Coverage in monolayers of exposed surface metal area.

It is important to point out here that the concentration (μmol g^{-1}) of active ''H-containing'' intermediate species reported in Table 1 for the WGS reaction at 350 °C is less than 4% of the theoretical maximum concentration (monolayer) of –OH and H species accommodated on the present γ-Al_2O_3 surface in its fully hydrated state (one –OH group on the Al cation and one H on the adjacent oxygen anion). This concentration was estimated to be 63 μmol (–OH and H) per m^2, or 9.3 mmol (–OH and H) per gram of alumina based on surface crystallographic data [35]. At the WGS reaction temperature of 500 °C, the concentration of active ''H-containing'' species is less than 35% of the monolayer value for all three catalysts investigated. It is also important to note that in the 350–500 °C range dehydration of γ-Al_2O_3 under vacuum leaves about 50–30% of the –OH monolayer [36,37]. In the present catalytic experiments the water partial pressure was 95 Torr, thus higher coverages for the –OH species must be expected.

The above-mentioned results point out that under the present WGS reaction conditions *not all* –OH groups present on the alumina surface are able to participate in the reaction path to form H_2 gas. Also, according to Martin and Duprez [38] only a small fraction of –OH groups is likely energetically able to diffuse towards a metal particle supported on a metal oxide considering a heterogeneous surface diffusion model. It is also very important from a mechanistic point of view to show that the large concentration of ''H-containing'' species measured in the SSITKA experiments (Fig. 2) cannot be justified as being present along the periphery of the metal-support interface. This can be illustrated after considering the following relationship [38]:

$$I_o = \alpha X_m D^2 \quad (5)$$

where, I_o is the total circumference of the noble metal particles (m g_{cat}^{-1}), X_m is the noble metal loading (wt%), and D is the dispersion (%) of noble metal. In the case of 0.5 wt% Rh/Al_2O_3 catalyst ($D = 47\%$), assuming hemispherical Rh particles ($\alpha = 8.8 \times 10^5$ (m g_{cat}^{-1}) [38]), and a distance between two adjacent OH groups of about 2 Å, the concentration of –OH groups present along the periphery of metal-support interface is estimated to be 8 μmol g_{cat}^{-1} to be compared to 138 and 1093 μmol g_{cat}^{-1} measured under SSITKA experiments (Table 1). This result shows unambiguously that there must be a region around each noble metal particle within which

active –OH/H species participate in the ''H-path'' of the WGS reaction. Similar results were obtained for the Pt/γ-Al_2O_3 and Pd/γ-Al_2O_3 catalysts.

The possibility of producing HD and H_2 due to exchange reactions of D_2O(g) with the surface –OH groups of the alumina support during SSITKA experiments (Fig. 2) was carefully examined. A 10% H_2O/Ar mixture was passed over the catalyst for 30 min, followed by a switch to the equivalent isotopic mixture (10% D_2O/Ar) at 350 °C. No production of any HD or H_2 gases was observed by mass spectrometry under the 10% D_2O/Ar gas mixture. The H_2/D_2 exchange over the present noble metal supported catalysts was also checked. The catalyst was first reduced in H_2 at 300 °C and then flushed in Ar flow. A switch to a 0.5% H_2/0.5% D_2/Ar mixture was then performed. A large signal of HD was recorded with mass spectrometry due to both H and D recombination on the noble metal, and exchange of D of D_2(g) with the H of –OH groups on the alumina support. The latter result implies that during the first 2 min of the transient (Fig. 2), where H_2 and D_2 are present in the gas phase, some HD via exchange reactions can be formed. However, this result *will not* affect the accuracy of the measurement of the concentration of ''H-containing'' active intermediates. This can only alter the shape of the HD response curve since the latter is now the result of the different kinetics of the WGS and H_2/D_2 and D_2/OH exchange reactions.

3.2.2. Determination of ''carbon-pool''

The SSITKA switch 3%^{12}CO/10% H_2O/Ar/He (30 min, T) → 3%^{13}CO/10% H_2O/Ar (T, t) at T = 350 and 500 °C was performed for the measurement of the concentration of active ''carbon-containing'' intermediate species, named ''C-pool''. The dynamic responses of $^{12}CO_2$, $^{13}CO_2$ and He obtained upon the isotopic switch are given in Fig. 3. A steady-state CO conversion of 9.5% is noted. A relatively fast decrease in the gas phase concentration of $^{12}CO_2$ and a simultaneous increase of $^{13}CO_2$ were observed. The concentration (μmol g^{-1}) of ''C-pool'' participating in the carbon-path of the WGS reaction from CO towards the CO_2 formation can be estimated based on

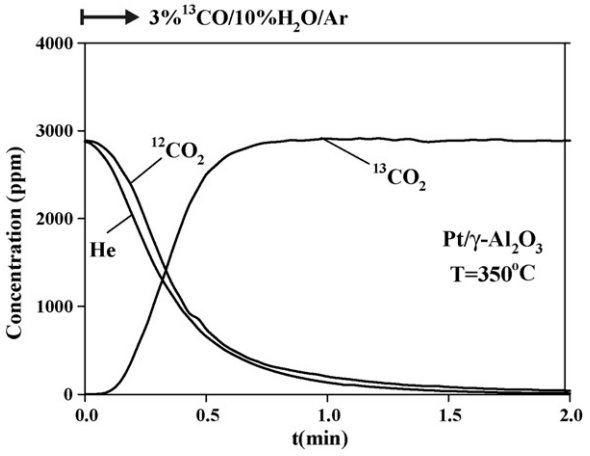

Fig. 3. SSITKA-mass spectrometry experiments performed to follow the ''C-path'' of WGS reaction over Pt/γ-Al_2O_3 at 350 °C according to the gas delivery sequence: 3%^{12}CO/10% H_2O/Ar/He (30 min) → 3%^{13}CO/10% H_2O/Ar (t).

the following relationship:

$$N_C(\mu\text{mol C}/g_{cat}) = \left(\frac{F_T}{W}\right)\left[\int_0^{t^f}(y_{CO_2} - y_{He})dt\right] \quad (6)$$

The concentration of ''C-pool'' estimated at T = 350 and 500 °C as well as the corresponding equivalent surface coverage, θ_C (based on the noble metal surface area) are given in Table 1. In contrast to the large concentration of ''H-pool'', the concentration in terms of θ_C of ''C-pool'' is less than 0.1 of a monolayer at 350 °C, and between 1.2 and 2.6 at 500 °C for the three alumina-supported noble metal catalysts. These results could imply that at 350 °C the active ''carbon-containing'' intermediate species are associated only with the metal surface. However, the possibility that all or part of it might be present on the support cannot be excluded. In fact, SSITKA-DRIFTS experiments of the WGS reaction provided evidence that active ''carbon-containing'' species found in the carbon-path of reaction at 350 and 500 °C consist of formate (–COOH) present on the alumina support and CO on the noble metal surface [29]. It is noted the absence of any ^{13}C isotopic effect according to the SSITKA results of Fig. 3.

The concentration of ''C-pool'' reported in Table 1 can justify only an equivalent amount of the ''H-pool'', if only active formate accumulates in the ''carbon-path'' under steady-state WGS reaction conditions. However, the presence of molecularly adsorbed CO [29] points out that the equivalent concentration of ''H-pool'' corresponding to formate species must be less than the concentration of ''C-pool'' reported in Table 1. Thus, it becomes clear that the ''H-pool'' measured cannot consist only of –COOH species but the vast majority of it comes from another active ''hydrogen-containing'' intermediate species (OH/H) as discussed in Section 3.2.1.

3.2.3. Kinetic isotopic effect

Based on the SSITKA results reported in Fig. 2, the rate of H_2(g) formation appears to be larger than that of D_2(g) by a factor of 2.1 and 1.8 at 350 °C and 500 °C, respectively, which implies the existence of a *normal kinetic isotopic effect* (KIE). A similar result has also been reported on various supported-Rh and -Pt catalysts [15,16,39,40]. The authors suggested that this result was consistent with formate (–COOH) decomposition being a likely rate-limiting step of the WGS reaction in accordance with other findings [41]. As will be shown in the following section, formate species were also identified by *in situ* DRIFTS studies of the WGS reaction on all the present alumina-supported noble metal catalysts. Formate was also identified as an *active intermediate* species on the present catalysts via SSITKA-DRIFTS studies (carbon isotopic shift of the O–C–O vibrational mode) [29]. Another elementary reaction step associated with the breaking of a chemical bond that involves H can also be considered to explain the normal KIE observed. For example, surface diffusion of H species (breaking of O–H bond) and water dissociation on the alumina surface might also be considered. However, based on reported values of the heat of adsorption for water on γ-Al_2O_3 [37], the

relatively high temperatures of reaction studied, the higher activation energy of formate decomposition compared to the heat of adsorption of water [37,42], and the lack of evidence in the literature that water dissociation could be considered as a rate-limiting step of the WGS reaction in the 350–500 °C range, water adsorption and dissociation steps on the alumina surface should not be considered to account for the normal KIE observed (Fig. 2). However, in the case of Pd metal [43], theoretical calculations have shown that water dissociation (26 kcal mol^{-1}) had the highest energy barrier among other steps considered in the reaction mechanism of WGS on Pd(1 1 1) surface. For the present alumina-supported noble metals, the WGS reaction could also proceed on the noble metal surface alone. However, it is not possible to quantify the individual rate of reaction taking place on the noble metal alone and that with the participation of alumina, as the present work has demonstrated. Concluding, water dissociation on the noble metal could only partly account for the deuterium KIE observed (Fig. 2).

3.3. In Situ DRIFTS (WGS reaction)

In situ DRIFTS spectra in the 3150–800 cm^{-1} range recorded over the 0.5 wt% Rh/γ-Al_2O_3 catalyst after 20 min of WGS reaction at 350 °C are shown in Fig. 4. The ir spectrum due to the stretching C–H vibrational mode of *formate* (–COOH) species is shown in Fig. 4a. The ir band centered at 2905 cm^{-1} corresponds to bidentate formate, while those centered at 2986 and 3060 cm^{-1} correspond to two different bridged formate species [14–16,18,39,44–46]. The latter assignment is consistent to the fact that formation of –COOH requires the participation of a surface –OH species [11], and γ-Al_2O_3 surface exposes three kinds of –OH groups [47] in a high degree of hydration. A similar spectrum to that shown in Fig. 4a was reported in the case of Pt/ThO_2 (WGS reaction) [39] and Rh/γ-Al_2O_3 (CO/H_2 reaction) [46]. In Fig. 4b the ir bands recorded at 2026 and 1968 cm^{-1} (after deconvolution) correspond to *linear CO*, and that at 1814 cm^{-1} to *bridged CO* [45,48–50].

Fig. 4c reports the ir spectrum in the 1700–1250 cm^{-1} range typical for the O–C–O stretching vibrational mode of *formate*, *carbonate* and *carboxylate* species [15,40,45,46]. In particular, the most intense bands recorded at 1594 and 1375 cm^{-1} are assigned to OCO_{as} and OCO_s of formate species, the ir band at 1533 cm^{-1} to OCO_{as} of carboxylate species, the ir band at 1483 cm^{-1} to OCO_{as} of unidentate carbonate, and the ir band at 1296 cm^{-1} to OCO_{as} of bidentate carbonate. The ir band recorded at 1650 cm^{-1} is suggested to be the result of the bending vibrational mode of molecularly adsorbed H_2O (∼1630–1650 cm^{-1}) and of the OCO_{as} of the bridged formate that gave the νCH band at 3060 cm^{-1}. Finally, the ir band centered at 821 cm^{-1} (Fig. 4d) corresponds to ionic carbonate (out of plane deformation mode) [45,51]. It is noted that the intensity of all the infrared bands reported in Fig. 4 were decreased as reaction temperature was increased to 500 °C. It is also noted that an ir band centered at 2345 cm^{-1} due to linearly adsorbed carbon dioxide on cus Al^{3+} cations (Lewis sites) [52], and a very broad ir band in the 3800–3300 cm^{-1} range assigned to –OH groups on the γ-alumina support [47] were also observed. Infrared bands due to a linear adsorbed CO_2 (2343 cm^{-1}) and molecularly adsorbed water (1640 cm^{-1}) on ceria were observed over Au/CeO_2 during WGS reaction conditions [53].

In situ DRIFTS spectra were also recorded over the Pt/γ-Al_2O_3 and Pd/γ-Al_2O_3 catalysts at the same reaction conditions. No additional ir bands that could be assigned to

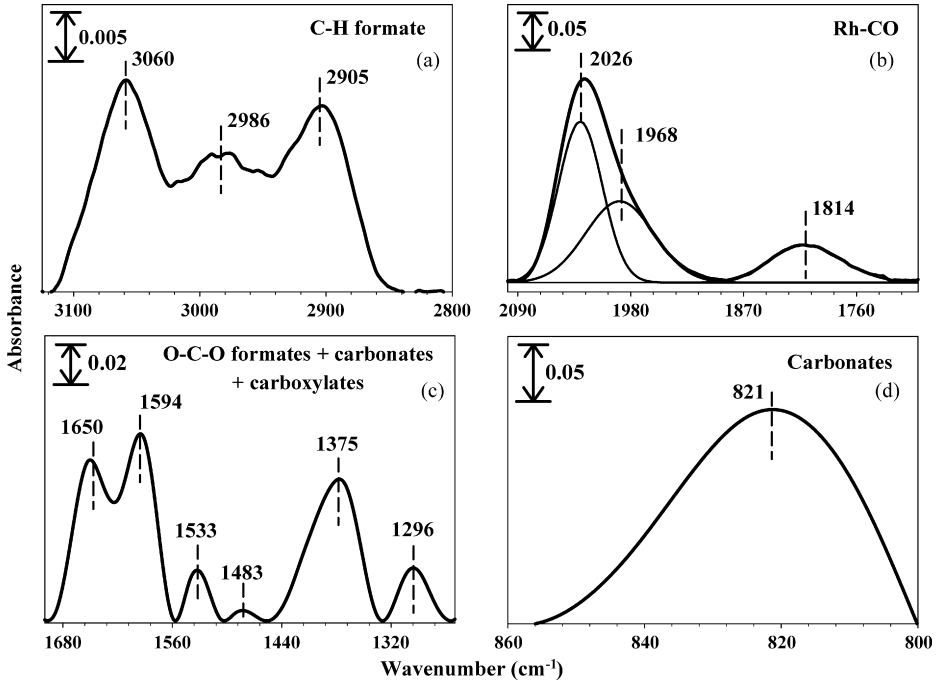

Fig. 4. *In situ* DRIFTS spectra recorded in the 3125–800 cm^{-1} range after 20 min of WGS reaction at 350 °C over the 0.5 wt% Rh/γ-Al_2O_3 catalyst. Infrared bands corresponding to adsorbed formate, carbonates, and carboxylate intermediate species on the alumina support, and linear/bridged CO on the Rh metal are shown.

different adsorbed species than those observed over Rh/γ-Al_2O_3 (Fig. 4) were noticed.

3.4. The catalytic chemistry of the WGS reaction over alumina-supported Rh, Pt and Pd

3.4.1. Chemical structure of active intermediate species and elementary reaction steps

The concentration of the active ''H-containing'' reaction intermediates as determined by SSITKA-mass Spectrometry experiments (Fig. 2, Table 1), and discussed in Section 3.2.1, along with the very small activity of γ-alumina alone at $T > 350$ °C (Fig. 1) strongly suggest that the reaction sequence must account for the role of both the support and the metal (Pt, Rh, Pd). In addition, the fact that γ-Al_2O_3 is an ''*irreducible*'' oxide at the reaction conditions investigated must exclude the ''redox'' mechanism extensively discussed in the literature [54–56] for ''reducible'' metal oxides and supported metal catalysts on such carriers. An alternative mechanism has been extensively discussed [11,16,18,57] according to which the WGS reaction proceeds via the interaction of adsorbed CO with terminal hydroxyl groups of the support to form formate species (–COOH), an active ''carbon-containing'' reaction intermediate which further reacts with an adjacent OH group on the support to form H_2(g) and carbonate adsorbed species. The latter decomposes to form CO_2(g).

In the case of alumina-supported metal catalysts, a reaction mechanism was proposed [19] according to which formation of adsorbed formate is due to the interaction of adsorbed CO on the metal and water molecule or –OH group on the alumina support. This reaction intermediate is then diffused (back spilt over) towards the metal, which decomposes rapidly into CO_2 and H_2 [19]. The latter step requires the abstraction of H from the formate species on the metal surface. Thus, the role of metal becomes apparent based on this elementary step.

In the following proposed mechanistic scheme, *formate species* (–COOH) formed on the alumina support is an active intermediate of the WGS reaction (Fig. 4, [29]) as also reported by SSITKA-DRIFTS studies on Pt/CeO_2 [11]. It has been reported [58,59] that formate species decomposes at very low temperatures on noble metal surfaces, thus its population in the 350–500 °C range under WGS reaction conditions appears very unlikely. In addition, molecularly adsorbed CO on the noble metal appears as an active intermediate species [29].

It is proposed that alumina support can activate the water molecule [35,36] according to the following elementary reaction steps:

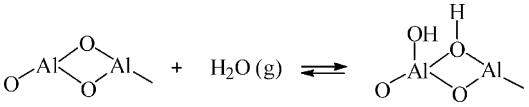

(7)

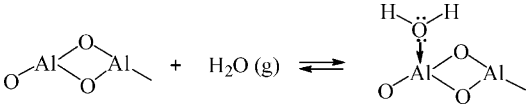

(8)

Reaction (7) is the dissociative adsorption of water onto the alumina support acid-base sites, whereas reaction (8) is the nondissociative adsorption of water on Lewis acid sites. Reaction step (8) is very unlikely to occur at high WGS reaction temperatures (e.g., $T \geq 300$ °C) [60]. Based on the catalytic activity results of Fig. 1, CO activation on the noble metal must be an important step, especially at temperatures lower than 400 °C. This elementary step is described by reaction (9):

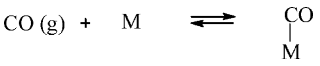

(9)

The chemisorption of CO is considered to be a reversible step (see Section 3.5). The formation of active formate (–COOH) species [29] is the result of reaction of adsorbed CO initially formed on the noble metal with the –OH groups present on the alumina support. Since the adsorption sites of these two species are different, it is rather clear that adsorbed CO *must diffuse* from the metal surface towards the –OH groups located on the alumina support (see Section 3.2.1) according to the following elementary step:

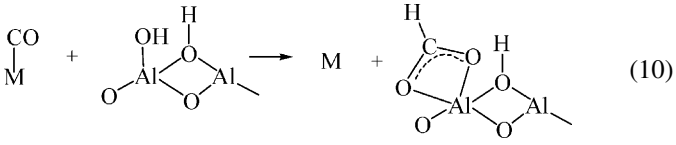

(10)

It is important to note that spillover of adsorbed CO from Pt and Pd to the alumina support at $T > 250$ °C was proved experimentally [61,62]. Given the fact that the concentration of active ''carbon-containing'' intermediate species does not exceed the value of about 2.5 equivalent monolayers of surface noble metal (Table 1, Section 3.2.2), it can be suggested that active formate species could also be located at the periphery of metal–support interface.

In order to produce CO_2(g) and H_2(g) from adsorbed –COOH species, it is necessary that formate reacts with an adjacent –OH group according to the elementary step (11):

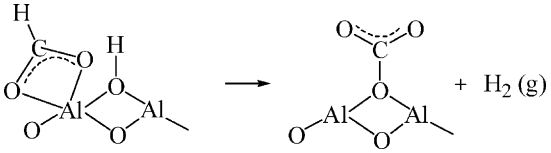

(11)

The produced adsorbed carbonate species is further decomposed to produce CO_2(g) according to the elementary step (12):

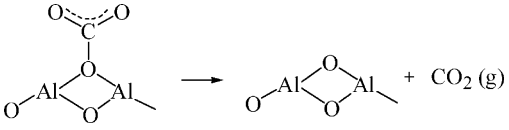

(12)

It has been suggested [12,19,39,63] that adsorbed formate on alumina can be decomposed with the aid of noble metal to CO_2(g) and atomic H, the latter recombining with an adjacent adsorbed H to form molecular H_2(g). It is difficult to envision the diffusion of formate species as entity (see reaction step (11)) towards the noble metal particles in order that formate get decomposed into CO_2(g) and adsorbed H species, even though

the latter step was suggested [58]. It is rather more reasonable to suggest that formate adsorbed on Al–O sites along the periphery of metal–support interface is able energetically to interact with the metal surface and get decomposed into CO_2(g) and adsorbed H product species.

As discussed in Section 3.2.1, –OH/H species located within a certain radii around a noble metal particle participate in the "hydrogen-path" of the WGS reaction. An important mechanistic issue which naturally then arises and needs to be discussed is whether the formation of active formate species is the result of *diffusion of CO* from the noble metal surface to the Al–OH support sites (reaction step (10)), *or the diffusion of –OH groups* from the alumina support towards adsorbed CO located along the circumference of the metal-support interface. Recently, Duprez et al. [12,38,63] have demonstrated the significance of surface diffusion steps of –OH groups and H species on supported-noble metal catalysts in the WGS and steam reforming reactions. In particular, the mechanism of migration of the OH/H species on metal oxide surfaces with basic and mild Brønsted acidic character (e.g., γ-Al_2O_3) has been illustrated.

The mobility of H species was extensively studied on noble metals supported on various metal oxides [12,38], where rates of surface diffusion and diffusivities were calculated. The surface diffusion of H species has been demonstrated on Rh/γ-Al_2O_3 diluted with γ-Al_2O_3 via H_2-TPD and toluene hydrogenation experiments [64]. The same phenomenon was also studied on Pd/γ-Al_2O_3 diluted with γ-Al_2O_3 using DSC measurements [65], and on Pt/γ-Al_2O_3 by electrical conductivity transient response methods [66]. However, to our knowledge no similar studies appear in the literature for –OH and CO diffusion on γ-Al_2O_3 alone or on alumina-supported noble metals. It is rather difficult to predict the relative diffusion rates of –OH and CO species based on arguments related only to the binding strength of these species with alumina surface sites. This important issue awaits experimental evidence. In the following section, the WGS reaction mechanism is presented and discussed via "compartmental modelling" [67–69] based on which the notion of OH/H diffusion being a slow reaction step could find support.

3.4.2. Interpretation of reaction mechanism via "compartmental modelling"

Scheme 1 illustrates the "H-path" and "C-path" of the WGS reaction in terms of a series of pools referred to as "compartmental modelling" [67–69]. Each pool represents a given reaction species (subscript s refers to a surface active intermediate species). The size of the pool reflects the concentration (μmol g^{-1}) of active intermediate species identified (Fig. 2, [29]). The pools are connected with pipes (hydraulic analogue), where the diameter of the pipe connecting two consecutive pools reflects the *rate constant* associated with the elementary reaction step which involves the two respective intermediate species [67–69]. The *rate-determining step* will be that associated with the pipe having the *smallest diameter*. As a result of this, the pool preceding this pipe will be expected to accumulate the largest amount of

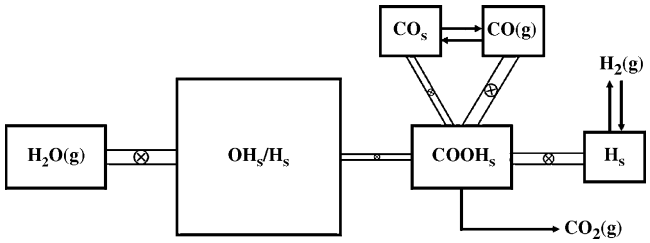

Scheme 1. Compartmental model representation of the hydrogen (H) and carbon (C) reaction paths followed during the water–gas shift reaction over alumina-supported Pt, Pd and Rh catalysts in the 350–500 °C range. The size (μmol g_{cat}^{-1}) of each pool corresponds to the concentration of reactant or active adsorbed intermediate species, while the size of each pipe connecting two consecutive pools reflects the magnitude of the kinetic rate constant associated with an elementary reaction step that involves the two respective intermediate species.

surface active intermediate species. According to the elementary reaction steps (7), (10) and (11), a pool of gaseous H_2O (∼55 μmol) (12.5 vol% was used in the feed stream, ∼3 mL gas-phase reactor volume, T = 350 °C) is connected with the –OH/H pool which supplies the pool of –COOH adsorbed species. It is noted here that formate species produced on the alumina surface alone during WGS reaction was also reported [42]. Formate species may lead to H adsorbed on the noble metal, if the latter is postulated to participate in the decomposition of formate. The last step in the "H-path" is the recombination of two adsorbed H species leading eventually to the H_2(g) product.

The fact that under steady-state reaction conditions the rate of water dissociation to form OH/H species must be equal to the rate of COOH formation via the participation of –OH groups, and also to the rate of formate decomposition to produce H_2(g), kinetic reasoning then implies that the accumulation of a large concentration of OH/H intermediate species is the result of a *small rate constant* (small pipe diameter in the compartmental modelling of Scheme 1) associated with a reaction step present between the two consecutive pools [67–69]. Thus, diffusion of –OH species towards active catalytic sites where adsorbed CO is formed could be considered as a slow step.

Under steady-state reaction conditions (SSITKA), the rate of diffusion of OH species must be equal to the rate of formate decomposition. If for simplicity it is assumed that:

$$\text{Rate} \sim k_{\text{d}}^{\text{app}}[\text{OH}] \sim k_{\text{app}}[\text{COOH}] \tag{13}$$

where $k_{\text{d}}^{\text{app}}$ is an apparent rate constant for surface diffusion, and k_{app} is an apparent rate constant for the reaction step of formate decomposition, then

$$[\text{OH}] \sim \left(\frac{1}{k_{\text{d}}^{\text{app}}}\right)[\text{COOH}]k_{\text{app}} \tag{14}$$

Based on Eq. (14), the establishment of a large concentration of active OH groups could be seen as the result of a small rate constant for surface diffusion of OH groups (small pipe diameter at the exit of OH/H pool shown in Scheme 1).

However, if surface diffusion of CO towards the –OH groups on the alumina support is assumed to take place, which could

also be considered as a slow step, then the large concentration of OH/H species measured under steady-state reaction conditions (Table 1) could be interpreted as the result of the significant activation of these species in the 350–500 °C range leading to their participation in the ''H-path'' of WGS reaction.

Below some important quantitative results derived from the SSITKA-mass spectrometry experiments (Table 1) are discussed.

(a) There is a significant increase in the concentration of active ''H-containing'' intermediates with reaction temperature for all three catalysts investigated. This result can be explained by either considering that –OH or CO diffusion is an important step. Surface diffusion is an activated process, and considering also the heterogeneous diffusion model reported by Duprez [38] for preferential diffusion paths, then the increase of reaction T is reasonably expected to increase the rate of diffusion and the participation of an increased concentration of that species to given elementary steps present in the reaction mechanism. The steady-state surface concentration of these species at a given reaction T is controlled by their rates of formation and consumption.

(b) There is an increase in the concentration of active ''C-containing'' intermediates with reaction temperature for all three catalysts investigated, where this increase remains much smaller than that observed for the ''H-pool''. It is suggested that this might be due to the increase of surface CO diffusion rate from the noble metal to the alumina support or the metal-support interface, where adsorbed CO is necessary to form active formate species. The increase of the latter rate appears to be larger than that of formate decomposition (step (11)). Activation of a second type of formate species towards decomposition by increasing the reaction T from 350 to 500 °C could be considered as another reasonable explanation. Support on this is provided by recent SSITKA-DRIFTS studies of the WGS reaction on a Pt/CeO_2 catalyst [70].

(c) Based on the results of Table 1, there is a clear dependence of the concentration (μmol g^{-1}) of the active ''H-pool'' and ''C-pool'' on the chemical nature of noble metal (Pt, Pd, Rh). This dependence is also clearly seen in the activity performance of the three supported-metal catalysts (Fig. 1). According to the previous discussion, one of the main roles of noble metal in the mechanism of WGS reaction is to *activate the CO molecule*. As will be shown in the following section, different in chemical structure and concentration of active CO adsorbed states are formed depending on the chemical nature of noble metal. It is reasonable to expect that the latter will affect the surface diffusion of CO from the noble metal to the alumina support, thus the rate of formation of formate species. Also, if for the present reaction mechanism the decomposition of formate by the aid of noble metal (active formate is located along the periphery of metal-support interface) is also an important slow reaction step, then the intrinsic differences in the surface electronic states of the three noble metals would be expected to influence the overall reaction rate (Fig. 1).

(d) At 500 °C, $Pd/\gamma\text{-}Al_2O_3$ accumulates OH/H species in a concentration about three times higher than $Rh/\gamma\text{-}Al_2O_3$ catalyst does (Table 1). It is noted that the two catalysts bare the same loading and dispersion, thus practically the same number of noble metal particles per gram of catalyst. It has been reported [71] that deposition of Pd atoms on the $\gamma\text{-}Al_2O_3$ carrier is preferential on a given type of Al sites, where local Al-O bond strengths are altered compared to Al–O bonds distant from the adsorbed Pd atom. Also, the role of OH groups of alumina on the growth and interaction with supported Rh clusters was reported [72]. Martin and Duprez [38] emphasized also the heterogeneous model of surface diffusion for a supported-metal catalyst according to which the concentration of surface diffused species will be restricted by the size of the ''gates'' and the metal/support interface. We suggest that all the above-mentioned factors could reasonably be considered responsible for the observed difference in the concentration of the active ''H-pool'' between $Pd/\gamma\text{-}Al_2O_3$ and $Rh/\gamma\text{-}Al_2O_3$ catalysts.

3.5. CO chemisorption studies

3.5.1. DRIFTS CO chemisorption at 25 °C

In situ DRIFTS spectra in the 2130–1760 cm^{-1} range obtained after CO chemisorption at 25 °C for 20 min over the 0.5 wt% $Rh/\gamma\text{-}Al_2O_3$ catalyst are presented in Fig. 5 (upper spectrum). After deconvolution [28] of regions of the spectrum (see lower spectrum, Fig. 5), linear and gem-dicarbonyl CO (2130–1960 cm^{-1} range) and two different kinds of bridged CO species (1920–1760 cm^{-1} range) were formed. The assignment of the structures of the various adsorbed CO species was based on literature data [46,48–51,73], and these are shown in the upper spectrum of Fig. 5. After using the integrated absorbance for each species following deconvolution of the recorded DRIFTS spectrum in Kubelka-Munk units, and the extinction coefficient (ε) of each adsorbed species [74,75], the percentage population of each kind of adsorbed CO on Rh can be calculated [75]. The results obtained are given in Table 2. In the case of $Rh/\gamma\text{-}Al_2O_3$ the most populated CO species is the

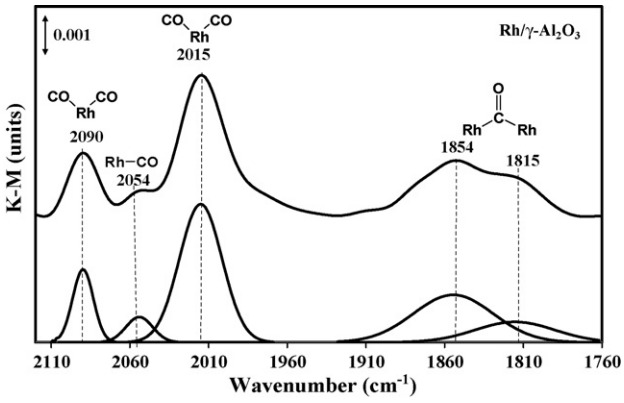

Fig. 5. *In situ* DRIFTS spectrum recorded in the 2130–1760 cm^{-1} range after 20 min of CO chemisorption at 25 °C over the $Rh/\gamma\text{-}Al_2O_3$ catalyst. Also shown (bottom graph) are the individual absorption bands of various adsorbed CO species obtained after deconvolution of the recorded spectrum.

Table 2
Distribution of various kinds of adsorbed CO on alumina-supported Pt, Pd and Rh (0.5 wt%) catalysts determined by CO chemisorption-DRIFTS studies at 25 °C. Also shown is the ratio of Linear/bridged CO after chemisortion at 25 °C and Water–gas shift reaction at 350 °C

Catalyst	M–CO species (%), adsorption of CO at 25 °C				CO adsorption (25 °C)	WGS reaction (350 °C)
	Gem-dicarbonyl	Linear	Bridged (2F co-ordinated)	Bidged (3F co-ordinated)	Linear/bridged (2F + 3F)	Linear/bridged (2F + 3F)
$Pt/\gamma\text{-}Al_2O_3$	–	37	33	30	0.6	0.6
$Rh/\gamma\text{-}Al_2O_3$	17	39	44	–	0.9	5.0
$Pd/\gamma\text{-}Al_2O_3$	–	34	3	63	0.5	0.3

bridged one (44%), whereas the least populated one is the gem-dicarbonyl CO (17%).

Fig. 6 presents similar ir spectra obtained over the $Pd/\gamma\text{-}Al_2O_3$ (a) and $Pt/\gamma\text{-}Al_2O_3$ (b) catalysts, while the percentage population of all kinds of CO species is provided in Table 2. Extinction coefficients for the linear and bridged (two-fold coordinated) adsorbed CO over the $Pt/\gamma\text{-}Al_2O_3$ and $Pd/\gamma\text{-}Al_2O_3$ catalysts were obtained from the literature [76,77], while the extinction coefficient for the three-fold coordinated CO was taken the same as that of two-fold coordinated CO. In the case of $Pd/\gamma\text{-}Al_2O_3$ (Fig. 6a), the ir bands at 2083 and 2055 cm^{-1} are assigned to two different linear CO adsorbed species [78–80] (after deconvolution, see Fig. 6a, bottom spectrum), the ir band at 1960 cm^{-1} is assigned to bridged CO [78,80], while those at 1865 and 1807 cm^{-1} to three-fold coordinated CO species [78,80]. The ir band at 2110 cm^{-1} is due to gaseous CO [51] (not presented in the deconvoluted spectrum at the bottom of Fig. 6a). In the case of $Pt/\gamma\text{-}Al_2O_3$ (Fig. 6b), the ir bands at 2057 and 2035 cm^{-1} are assigned to two different linear adsorbed CO species [81,82], while the ir bands at 1834 and 1767 cm^{-1} to bridged CO [82,83], and that at 1805 cm^{-1} to three-fold coordinated CO [82].

3.5.2. DRIFTS CO under WGS reaction conditions

Fig. 7 shows recorded ir spectra in the region of the C–O stretching vibrational mode of adsorbed CO after 20 min of

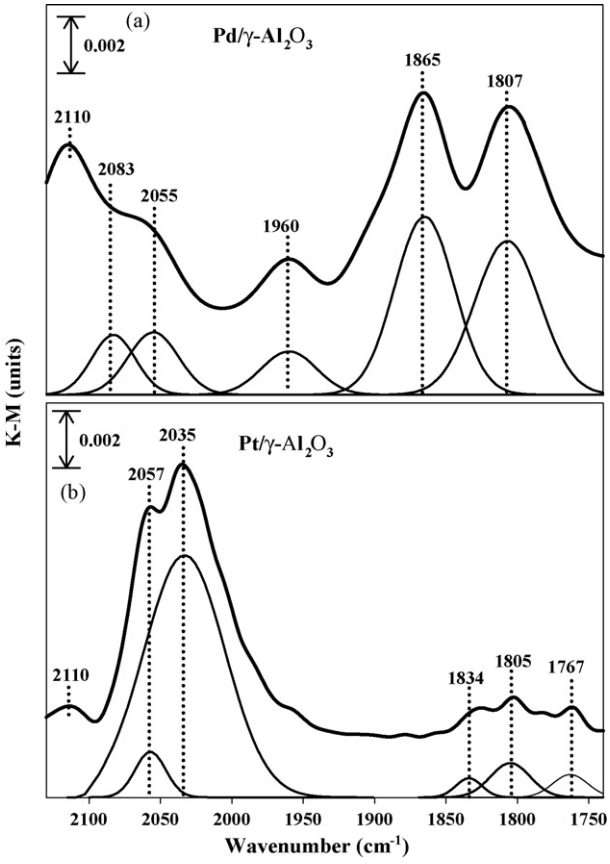

Fig. 6. *In situ* DRIFTS spectra recorded in the 2150–1740 cm^{-1} range after 20 min of CO chemisorption at 25 °C over the $Pd/\gamma\text{-}Al_2O_3$ (a) and $Pt/\gamma\text{-}Al_2O_3$ (b) catalysts. Also shown (bottom graph) are the individual absorption bands of various adsorbed CO species obtained after deconvolution of the recorded spectrum.

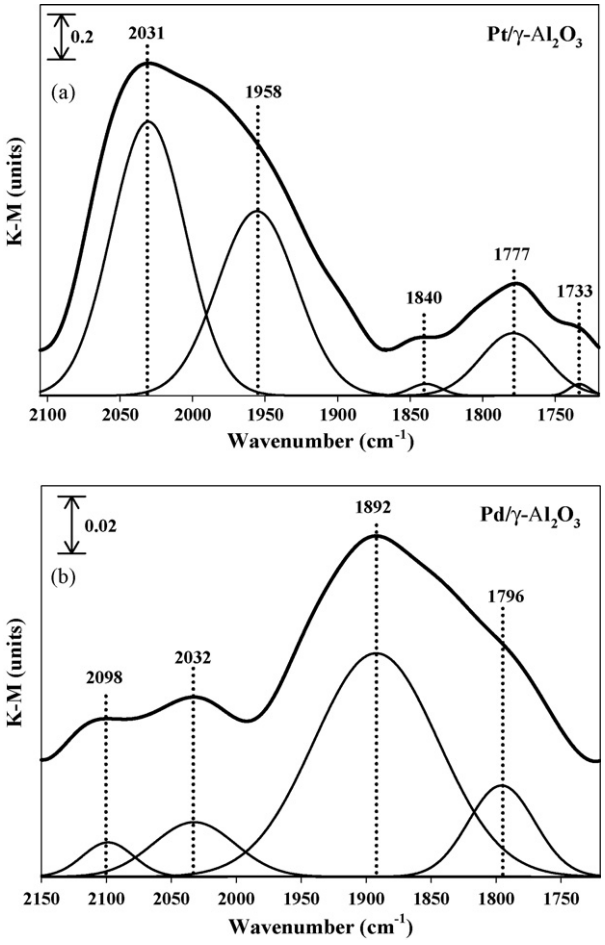

Fig. 7. *In situ* DRIFTS spectra recorded in the 2140–1720 cm^{-1} range after 20 min of WGS reaction at 350 °C over the $Pt/\gamma\text{-}Al_2O_3$ (a) and $Pd/\gamma\text{-}Al_2O_3$ (b) catalysts. Also shown (bottom graph) are the individual absorption bands of various adsorbed CO species obtained after deconvolution of the recorded spectrum.

WGS reaction at 350 °C over the Pt/γ-Al_2O_3 (Fig. 7a) and Pd/γ-Al_2O_3 (Fig. 7b) catalysts. Also shown are the various individual CO absorption bands obtained after spectra deconvolution. In the case of Pt/γ-Al_2O_3, most of the ir bands (linear + bridged CO) were shifted to lower wavenumbers compared to the case of CO chemisorption (absence of H_2O) at 25 °C (Fig. 6), where the opposite result was seen in the case of Pd/γ-Al_2O_3 catalyst (Fig. 7b). The former behavior is clearly illustrated in Fig. 8 where the individual CO absorption bands obtained after deconvolution of the original spectra are compared. It is seen that under the WGS reaction conditions a new adsorbed state of linear CO (1958 cm^{-1}) not populated in the absence of water (see Fig. 8b) is present. The appearance of this adsorbed state of CO is positioned 73 cm^{-1} lower than the main ir band observed at 2031 cm^{-1}, the latter present also at the same position following CO chemisorption at 25 °C. This result cannot be due to the effect of surface coverage of CO or of some carbon likely formed under the WGS reaction conditions. For Pt(1 0 0) and Pt(1 1 1) surfaces a shift by 40 cm^{-1} was observed in the ir band of adsorbed CO as the coverage of CO varied from zero to a monolayer value [84]. Also, in the case of Rh(1 1 1) [85] and Ni/γ-Al_2O_3 [86] surfaces precovered by carbon, only a slight shift (less than 30 cm^{-1}) in the vibrational frequency of adsorbed CO was reported. On the other hand, the binding energy of the various bridged adsorbed CO species (1700–1850 cm^{-1} range) does not seem to be altered under the two gas atmospheres and reaction temperatures. There is only a small red shift of two of the bridged CO species (compare Fig. 8a and b).

After considering the integrated absorbance of a given CO adsorbed species for the two catalysts (Fig. 7), and the fact that for the linear CO the ratio of the extinction coefficient for Pt to that for Pd is 1.9, and for the bridged CO is 20.8, it is concluded that the concentration of adsorbed CO on Pt/γ-Al_2O_3 is significantly larger than that on Pd/γ-Al_2O_3. This result is valid assuming that the exctinction coefficients of adsorbed CO on a clean Pt and Pd metal surfaces change only to a small extent by the presence of other adsorbed species formed during the WGS reaction. Thus, it could be stated that this kinetic parameter of surface concentration of adsorbed CO (θ_{CO}) could be considered as one of the kinetic reasons that explain the significant activity of Pt/γ-Al_2O_3 compared to Pd/γ-Al_2O_3 catalyst (Fig. 1) according also to the discussion offered in Section 3.4.

3.5.3. CO chemisorption at 25 °C followed by TPD-mass spectrometry

Figs. 9–11 present CO TPD response curves for the three 0.5 wt% *M*/γ-Al_2O_3 catalysts (*M* = Rh, Pd or Pt) following chemisortion of CO at 25 °C. In the case of Rh/γ-Al_2O_3 catalyst (Fig. 9), three distinct CO desorption peaks were observed with peak maxima at 62, 191 and 300 °C. The large desorption peaks of CO are assigned to the linear and bridged CO species according to the *in situ* DRIFTS CO chemisorption studies (Table 2). In addition to desorbed CO, carbon dioxide also desorbed (see Fig. 9) and very small amounts of molecular hydrogen. It is well known [87] that CO adsorption on noble metals can cause the formation of CO_2 and ''carbon'' through

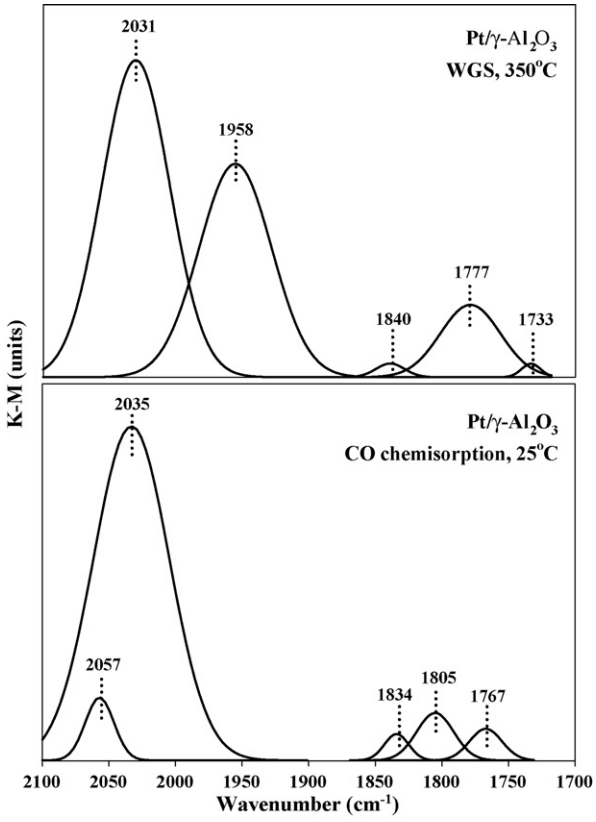

Fig. 8. Comparative absorption bands of various adsorbed CO species obtained under WGS reaction conditions (a) and CO chemisorption at 25 °C (b) on the 0.5 wt% Pt/γ-Al_2O_3 catalyst.

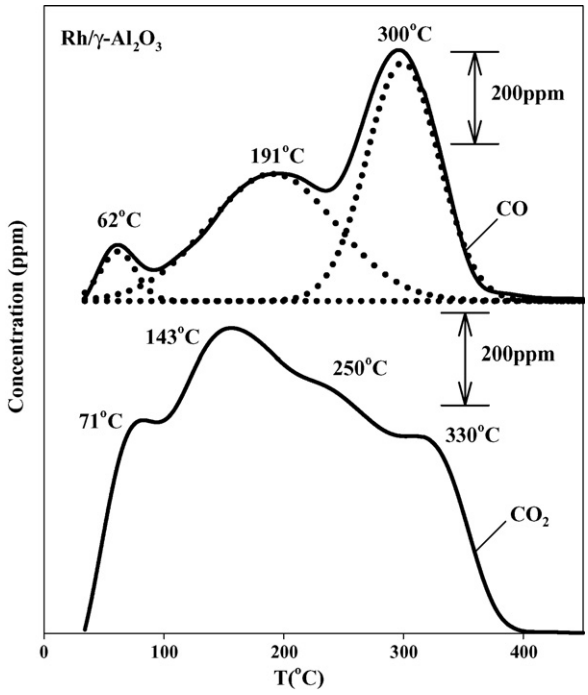

Fig. 9. Temperature-programmed desorption (TPD) response curves of CO and CO_2 obtained over 0.5 wt% Rh/γ-Al_2O_3 catalyst following CO adsorption at 25 °C. Q_{He} = 30 NmL min^{-1}; β = 30 °C min^{-1}; *W* = 0.3 g.

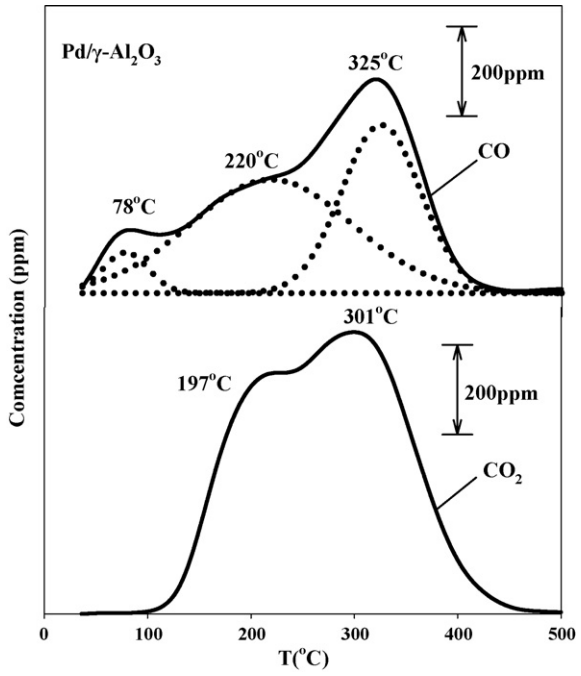

Fig. 10. Temperature-programmed desorption (TPD) response curves of CO and CO_2 obtained over 0.5 wt% Pd/γ-Al_2O_3 catalyst following CO adsorption at 25 °C. Q_{He} = 30 NmL min^{-1}; β = 30 °C min^{-1}; W = 0.3 g.

the Boudouard reaction:

$$2\,CO_{ads} \rightarrow C_{ads} + CO_2(g) \quad (15)$$

Additionally, adsorbed CO on the metal surface can potentially react with surface hydroxyl groups of the metal oxide support located at the periphery of the metal-support interface to form carbon dioxide and molecular hydrogen according to the following reaction [88]:

$$CO_{ads} + OH_L \rightarrow CO_2(g) + \tfrac{1}{2}H_2(g) \quad (16)$$

In the present work, the existence of reaction (16) proceeds to a small extent since small amounts of H_2 were detected. In fact, the low-temperature peak of CO_2 (T_M = 71 °C) is the result of reaction step (16) and not of reaction step (15), where a similar low-temperature CO_2 peak was also reported on a 5 wt% Rh/γ-Al_2O_3 catalyst [68]. It was reported [85] that adsorption of CO on Rh(1 1 1) precovered by carbon affected its TPD peak position by only 10 °C. This result allows to suggest that the adsorbed states of CO were only slightly affected by the carbon deposited (reaction step (15)).

Table 3 reports the concentration (μmol g^{-1}) and the equivalent surface coverage of adsorbed CO (in terms of monolayers of Rh_s). Based on the quantitative DRIFTS results reported in Table 2, and the fact that the alumina support alone chemisorbs 5.5 μmol CO g^{-1}, or θ = 0.23 (Table 3), it is likely that some new CO adsorption sites at the metal-support interface could have been created.

Figs. 10 and 11 present CO-TPDs for the Pd/γ-Al_2O_3 and Pt/γ-Al_2O_3 catalyst, respectively. It is seen that the temperature of maximum desorption rate, the concentration of the various desorbed CO species, and the kinetics of the Boudouard reaction all depend on the nature of noble metal. The total amount of adsorbed CO estimated and the peak maximum temperatures (T_{max}) observed are given in Table 3. In the case of Pt/γ-Al_2O_3 the total surface coverage of CO was practically the same as in the case of Rh/γ-Al_2O_3, and a similar explanation could be offered. However, based on the work of Flesner and Falconer [61] a spillover of CO on the alumina support may not be excluded. The large differences in the population of adsorbed CO as a function of the nature of noble metal as revealed by the *in situ* DRIFTS studies (Table 2) find good agreement with the CO-TPDs obtained by mass spectrometry. The T_{max} behavior (Table 3) allows also to conclude that the binding energy of adsorbed CO related to the surface of the three noble metals follows the order: Pd–CO > Rh–CO > Pt–CO. This result is in harmony with reported experimental results on the heat of adsorption of CO on unsupported Pt, Rh and Pd [89]. On the other hand, the catalytic activity of the

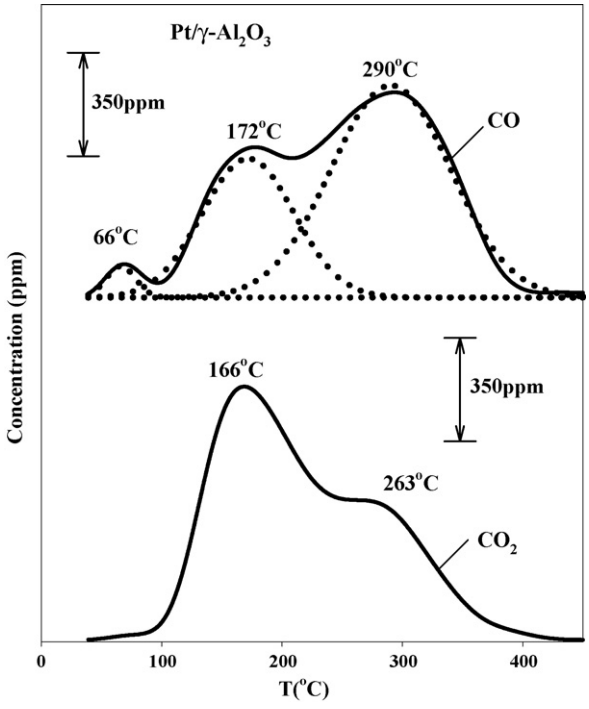

Fig. 11. Temperature-programmed desorption (TPD) response curves of CO and CO_2 obtained over 0.5 wt% Pt/γ-Al_2O_3 catalyst following CO adsorption at 25 °C. Q_{He} = 30 NmL min^{-1}; β = 30 °C min^{-1}; W = 0.3 g.

Table 3
Concentration of adsorbed CO (μmol CO g_{cat}^{-1}) and its equivalent surface coverage (θ_{CO}) estimated from TPD-CO experiments on 0.5 wt% M/γ-Al_2O_3 (M = Pt, Rh and Pd) catalysts. The peak maximum desorption temperatures (T_{max}) determined after deconvolution of CO-TPD curves are also given

Catalyst	Amount adsorbed (μmol CO g_{cat}^{-1})	T_{max} (1)[a] (°C)	T_{max} (2)[a] (°C)	T_{max} (3)[a] (°C)
Pt/γ-Al_2O_3	38.2 (θ = 2.2)[b]	66	172	290
Rh/γ-Al_2O_3	50.6 (θ = 2.1)[b]	62	191	300
Pd/γ-Al_2O_3	30.1 (θ = 1.3)[b]	78	220	325
γ-Al_2O_3	5.5 (θ = 0.23)[b]	375	–	–

[a] Desorption temperatures obtained after deconvolution of CO-TPD curves.
[b] θ = 1 corresponds to a monolayer surface coverage based on the noble metal area (CO/M_s = 1).

WGS reaction (Fig. 1) shows exactly the opposite trend. In other words, Pt supported on γ-Al_2O_3 with the lower binding energy of chemisorbed CO exhibits the highest catalytic activity, while Pd supported on γ-Al_2O_3 with the larger binding energy of chemisorbed CO exhibits the lowest catalytic activity. This result correlates with the fact that diffusion of CO from the noble metal to the alumina support surface might be an important elementary step of the WGS reaction (see Section 3.4).

4. Conclusions

The following main conclusions can be derived from the results of the present work:

- WGS reaction with a high H_2O/CO ratio (4:1 v/v) in the 350–500 °C range over alumina-supported Pt, Rh or Pd passes through a large concentration (μmol g^{-1}) of active OH/H species located on the alumina support and much smaller concentrations of active adsorbed CO (on the noble metal) and formate (on the alumina support) species.
- The accumulation of a large concentration of OH/H species on the alumina support during steady-state WGS reaction conditions on alumina-supported Pt, Rh or Pd may imply a small rate constant associated with the diffusion of these species towards catalytic sites present in the ''H-path'' of reaction mechanism.
- The large difference in the activity order of alumina-supported Pt, Rh or Pd metals (Pd < Rh < Pt) seems to correlate with the surface coverage of CO formed on the noble metal under WGS reaction conditions ($\theta_{CO}^{Pd} < \theta_{CO}^{Pt}$).
- TPD of CO and catalytic studies revealed that Pt/Al_2O_3 with a lower binding energy of chemisorbed CO compared to Pd/Al_2O_3 exhibits significantly larger WGS reaction activity.

Acknowledgements

We acknowledge the financial support by the European Committee (6th FP, no. 5183309 (SES6)) and the Research Committee of the University of Cyprus.

References

[1] D.S. Newsome, Catal. Rev. Sci. Eng. 21 (1980) 275.
[2] R.D. Cortright, R.R. Davda, J.A. Dumesic, Nature 418 (2002) 964.
[3] S. Chernik, R. French, C. Feik, E. Chornet, Ind. Eng. Chem. Res. 41 (2002) 4209.
[4] A.C. Basagiannis, X.E. Verykios, Appl. Catal. A: Gen. 308 (2006) 182.
[5] Q. Fu, H. Saltsburg, M. Flytzani-Stephanopoulos, Science 301 (2003) 935, and references therein.
[6] T.V. Choudhary, D.W. Goodman, Catal. Today 77 (2002) 65.
[7] T. Chapman, Physics World, July (2002).
[8] C. Rhodes, B. Peter Williams, F. King, G.J. Hutchings, Catal. Commun. 3 (2002) 381.
[9] R. Farrauto, S. Hwang, L. Shore, W. Ruettinger, J. Lampert, T. Giroux, Y. Liu, O. Ilinich, Annu. Rev. Mater. Res. 33 (2003) 1.
[10] A.B. Mhadeshwar, D.G. Vlachos, Catal. Today 105 (2005) 162.
[11] G. Jacobs, A.C. Crawford, B.H. Davis, Catal. Lett. 100 (2005) 147, and references therein.
[12] D. Duprez, Catal. Today 112 (2006) 17, and references therein.
[13] T. Shido, K. Asakura, Y. Iwasawa, J. Catal. 122 (1990) 55.
[14] T. Shido, Y. Iwasawa, J. Catal. 129 (1991) 343.
[15] T. Shido, Y. Iwasawa, J. Catal. 136 (1992) 493.
[16] T. Shido, Y. Iwasawa, J. Catal. 141 (1993) 71, and references therein.
[17] E. Chenu, G. Jacobs, A.C. Crawford, R.A. Keogh, P.M. Patterson, D.E. Sparks, B.H. Davis, Appl. Catal. B 59 (2005) 45.
[18] G. Jacobs, L. Williams, U. Graham, G.A. Thomas, D.E. Sparks, B.H. Davis, Appl. Catal. A: Gen. 252 (2003) 107.
[19] D.C. Grenoble, M.M. Estadt, D.F. Ollis, J. Catal. 67 (1981) 90, and references therein.
[20] A.M. Efstathiou, X.E. Verykios, Appl. Catal. A: Gen. 151 (1997) 109, and references therein.
[21] D. Tibiletti, A. Goguet, D. Reid, F.C. Meunier, R. Burch, Catal. Today 113 (2006) 94.
[22] A. Goguet, F.C. Meunier, D. Tibiletti, J.P. Breen, R. Burch, J. Phys. Chem. B 108 (2004) 20240.
[23] G. Jacobs, B. Davis, Appl. Catal. A 284 (2005) 31.
[24] C.N. Costa, A.M. Efstathiou, J. Phys. Chem. B 108 (2004) 2620.
[25] D.M. Stockwell, A. Bertucco, G.W. Coulston, C.O. Bennett, J. Catal. 113 (1988) 317, and references therein.
[26] P.C. Aben, J. Catal. 10 (1968) 224.
[27] C.N. Costa, T. Anastasiadou, A.M. Efstathiou, J. Catal. 194 (2000) 250.
[28] B.C. Smith, Fundamentals of fourier transform infrared spectroscopy, CRC Press, 1996.
[29] C.M. Kalamaras, G.G. Olympiou, A.M. Efstathiou, J. Catal., in preparation.
[30] K. Polychronopoulou, C.N. Costa, A.M. Efstathiou, Appl. Catal. A: Gen. 272 (2004) 37.
[31] Y. Choi, H.G. Stenger, J. Power Sources 124 (2003) 432.
[32] P. Panagiotopoulou, D.I. Kondarides, J. Catal. 225 (2004) 327.
[33] P. Panagiotopoulou, D.I. Kondarides, Catal. Today 112 (2006) 49.
[34] K. Polychronopoulou, A.M. Efstathiou, Catal. Today 116 (2006) 341.
[35] A. Ionescu, A. Allouche, J.-P. Aycard, M. Rajzmann, F. Hutschka, J. Phys. Chem. B 106 (2002) 9359.
[36] J.B. Peri, J. Phys. Chem. 69 (1965) 211.
[37] B.A. Hendriksen, D.R. Pearce, R. Rudham, J. Catal. 24 (1972) 82.
[38] D. Martin, D. Duprez, J. Phys. Chem. B 101 (1997) 4428.
[39] G. Jacobs, A. Crawford, L. Williams, P.M. Patterson, B.H. Davis, Appl. Catal. A: Gen. 267 (2004) 27.
[40] G. Jacobs, S. Khalid, P.M. Patterson, L. Williams, D. Sparks, B.H. Davis, Appl. Catal. A: Gen. 268 (2004) 255.
[41] G. Jacobs, P.M. Patterson, U.M. Graham, D.E. Sparks, B.H. Davis, Appl. Catal. A: Gen. 269 (2004) 63.
[42] (a) Y. Amenomiya, J. Catal. 57 (1979) 64;
(b) Y. Amenomiya, J. Catal. 55 (1978) 205.
[43] A.T. Bell, in: E. Shustorovich (Ed.), Metal-Surface Reaction Energetics,, VCH, 1991, chapter 5.
[44] C. Li, K. Domen, K.-I. Maruya, T. Onishi, J. Catal. 125 (1990) 445.
[45] G. Busca, J. Lamotte, J.-C. Lavalley, V. Lorenzelli, J. Am. Chem. Soc. 109 (1987) 5197.
[46] A.M. Efstathiou, T. Chafik, D. Bianchi, C.O. Bennett, J. Catal. 148 (1994) 224, and references therein.
[47] A.A. Tsyganenko, V.N. Filimonov, J. Mol. Struct. 19 (1973) 579.
[48] C.W. Rice, S.D. Worley, J. Chem. Phys. 74 (1981) 6487.
[49] F. Solymosi, M. Pasztor, J. Phys. Chem. 89 (1985) 4789.
[50] D.I. Kondarides, T. Chafik, X.E. Verykios, J. Catal. 191 (2000) 147.
[51] L.H. Little, IR Spectra of Adsorbed Species, Academic Press, New York, 1966.
[52] C. Morterra, G. Magnacca, Catal. Today 27 (1996) 497.
[53] T. Tabakova, F. Boccuzzi, M. Manzoli, D. Andreeva, Appl. Catal. A: Gen. 252 (2003) 385.
[54] T. Bunluesin, R.J. Gorte, G.W. Graham, Appl. Catal. B: Environ. 15 (1998) 107.
[55] Y. Li, Q. Fu, M. Flytzani-Stephanopoulos, Appl. Catal. B: Environ. 27 (2000) 179.
[56] F. Boccuzzi, A. Chiorino, M. Manzoli, D. Andreeva, T. Tabakova, J. Catal. 188 (1999) 176.

[57] G. Jacobs, L. Williams, U. Graham, D. Sparks, B.H. Davis, J. Phys. Chem. B 107 (2003) 10398.
[58] F. Solymosi, A. Erdöhelyi, J. Catal. 91 (1985) 327, and references therein.
[59] C. Egawa, I. Doi, S. Naito, K. Tamaru, Surf. Sci. 176 (1986) 491.
[60] K.C. Hass, W.F. Schneider, J. Phys. Chem. B 104 (2000) 5527.
[61] R.L. Flesner, J.L. Falconer, J. Catal. 139 (1993) 421.
[62] E.C. Hsiao, J.L. Falconer, J. Catal. 132 (1991) 145.
[63] J. Barbier Jr., D. Duprez, Appl. Catal. B: Environ. 4 (1994) 105.
[64] F. Benseradj, F. Sadi, M. Chater, Appl. Catal. A: Gen. 228 (2002) 135.
[65] M.V. Susic, J. Mater. Sci. 27 (1992) 3733.
[66] M. Stoica, M. Caldararu, F. Rusu, N.I. Ionescu, Appl. Catal. A: Gen. 183 (1999) 287.
[67] (a) D.M. Stockwell, C.O. Bennett, J. Catal. 110 (1988) 354;
(b) D.M. Stockwell, J.S. Chung, C.O. Bennett, J. Catal. 112 (1988) 135.
[68] A.M. Efstathiou, C.O. Bennett, J. Catal. 120 (1989) 137.
[69] J. Happel, Isotopic Assessment of Heterogeneous Catalysis, Academic Press, Inc., N.Y, 1986.
[70] F.C. Meunier, D. Tibiletti, A. Goguet, S. Shekhtman, C. Hardacre, R. Burch, Catal. Today, in press (available online).
[71] M.C. Valero, M. Digne, P. Sautet, P. Raybaud, Oil Gas Sci. Technol. 61 (2006) 535.
[72] M. Heemeier, M. Frank, J. Libuda, K. Wolter, H. Kuhlenbeck, M. Bäumer, H.-J. Freund, Catal. Lett. 68 (2000) 19.
[73] A.C. Yang, C.W. Garland, J. Phys. Chem. 61 (1957) 1504.
[74] P.B. Rasband, W.C. Hecker, J. Catal. 139 (1993) 551.
[75] T. Beutel, O.S. Alekseev, Y.U. Ryndin, V.A. Likholobov, H. Knözinger, J. Catal. 169 (1997) 132.
[76] M.A. Vannice, C.C. Twu, J. Chem. Phys. 75 (1981) 5944.
[77] M.A. Vannice, S.-Y. Wang, J. Phys. Chem. 85 (1981) 2543.
[78] D. Tessier, A. Rakai, F. Bonzon-Verduraz, J. Chem. Soc., Faraday Trans. 88 (1992) 741.
[79] K. Almusaiter, S.S.C. Chuang, J. Catal. 180 (1998) 161.
[80] A.M. Bradshaw, H. Hoffman, Surf. Sci. 72 (1978) 513.
[81] J. Rasko, J. Catal. 217 (2003) 478.
[82] A. Bourane, O. Dulaurent, D. Bianchi, J. Catal. 196 (2000) 115.
[83] R. Barth, R. Pitchai, R.L. Anderson, X.E. Verykios, J. Catal. 116 (1989) 61.
[84] A. Crossley, D.A. King, Surf. Sci. 95 (1980) 131.
[85] L.H. Dubois, G.A. Somorjai, Surf. Sci. 91 (1980) 514.
[86] J. Galuszka, J.R. Chang, Y. Amenomiya, J. Catal. 68 (1981) 172.
[87] R.W. McCabe, L.D. Schmidt, Surf. Sci. 60 (1976) 85.
[88] T. Ioannides, X. Verykios, J. Catal. 140 (1993) 353.
[89] M.A. Vannice, J. Catal. 50 (1977) 228.